

## Supporting Information

### **In situ growth of fluorescent silicon nanocrystals in monolithic microcapsule as a photostable, versatile platform**

*Guixian Zhu<sup>ab</sup>, Yu Huang<sup>c</sup>, Gauri Bhav<sup>b</sup>, Yuzhen Wang<sup>b</sup>, Zhongbo Hu<sup>a</sup>, and Xuewu Liu<sup>b\*</sup>*

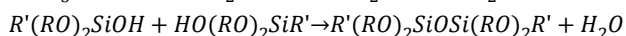
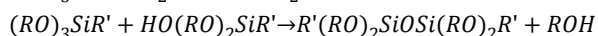
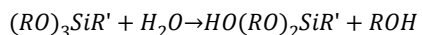
a. College of Materials Sciences and Opto-Electronics, University of Chinese Academy of Sciences, Beijing 100049, China

b. Department of Nanomedicine, Houston Methodist Research Institute, Houston, TX 77030, USA

c. Department of Biomedical Engineering, University of South Dakota, Sioux Falls, SD 57107 (USA)

\*Corresponding to: [xliu@houstonmethodist.org](mailto:xliu@houstonmethodist.org), Houston Methodist Research Institute, 6670 Bertner Ave, Houston, TX 77030, USA

#### **Equation S1**



Where R' stands for aminopropyl side chain, and R represents ethyloxy group on APTES.

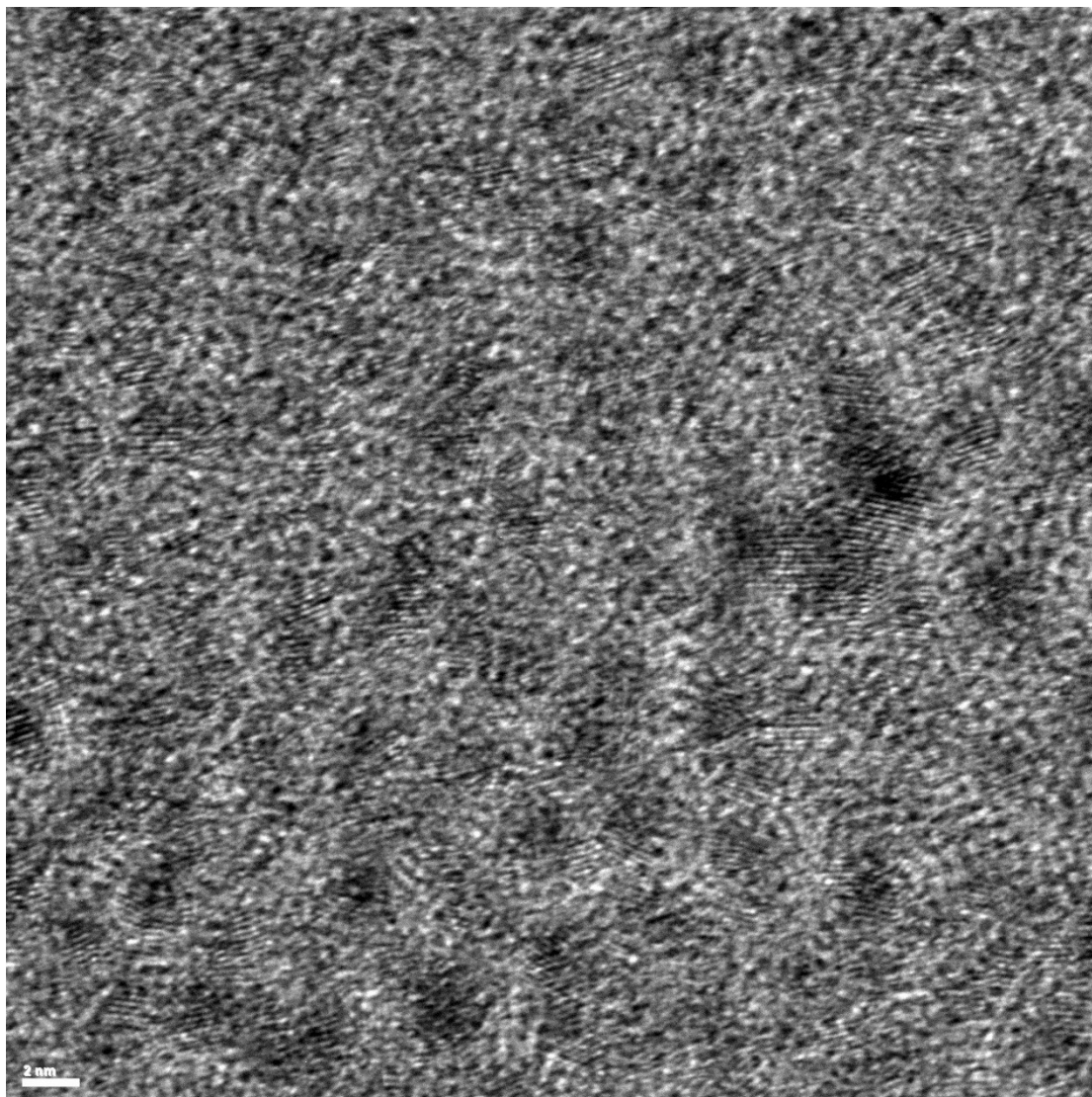


Fig. S1 TEM image of SiPM slices (70nm, cut by ultramicrotome) with well-distributed SiNC inside.

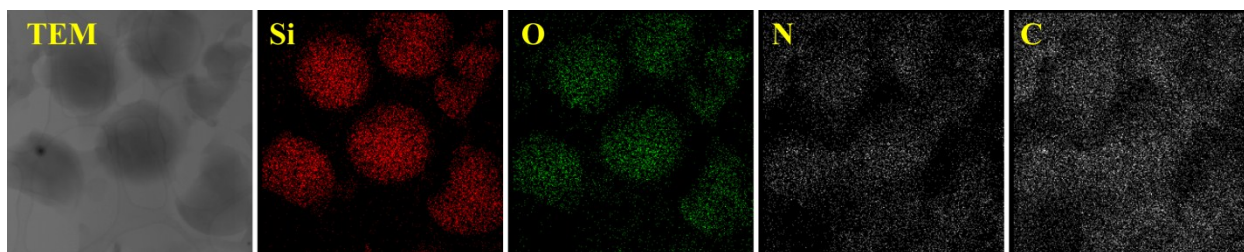


Fig. S2 EDS elemental mapping images for prepared SiPM slices (70nm, cut by ultramicrotome)

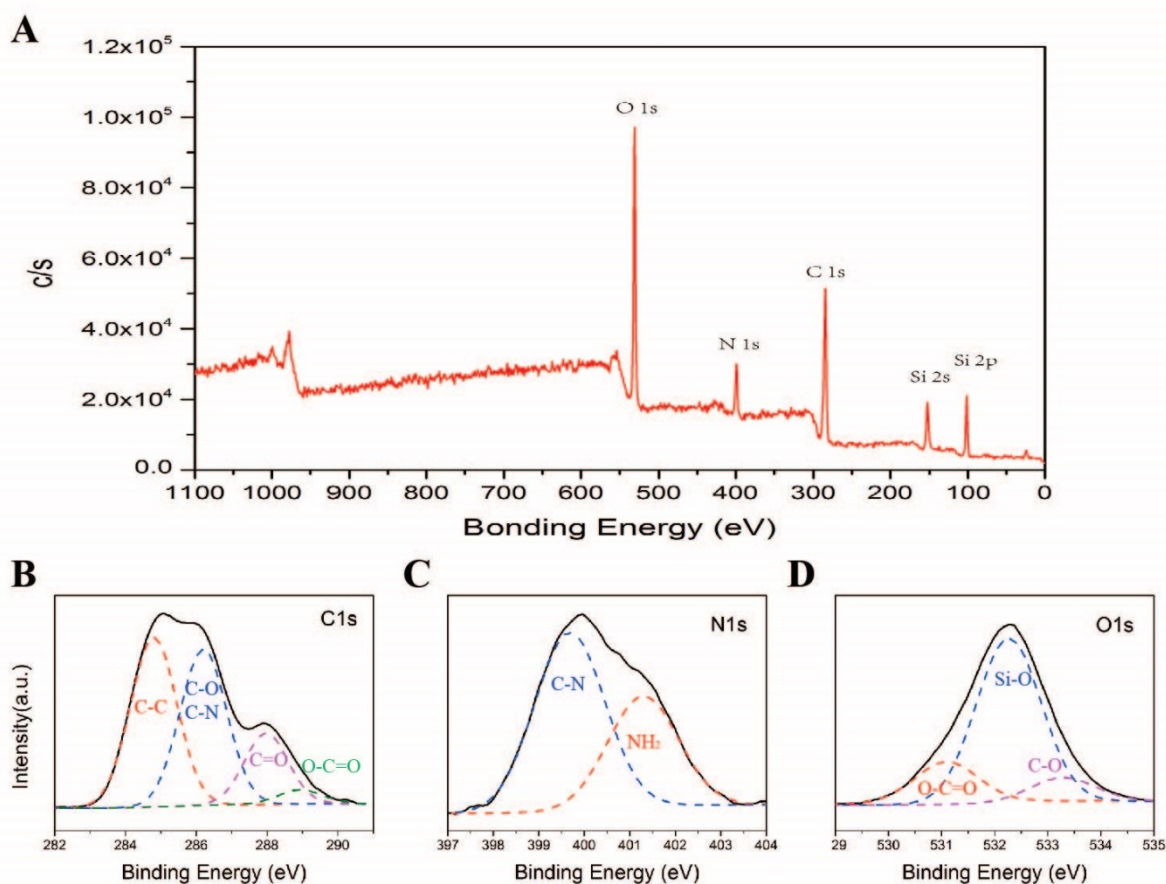


Fig. S3. XPS spectrum of SiPM (A), and structure analysis of high resolution XPS spectra: (B) C1s, (C) N1s and(D) O1s

The high resolution XPS spectra indicate that various chemical bonds are contained in SiPM such as C-C, C-N, C-O, C=O and Si-O. The C=O may come from ascorbic acid in polymer matrix. The existence of Si-O, C-N and NH<sub>2</sub> is attributed to siloxane matrices derived from APTES.

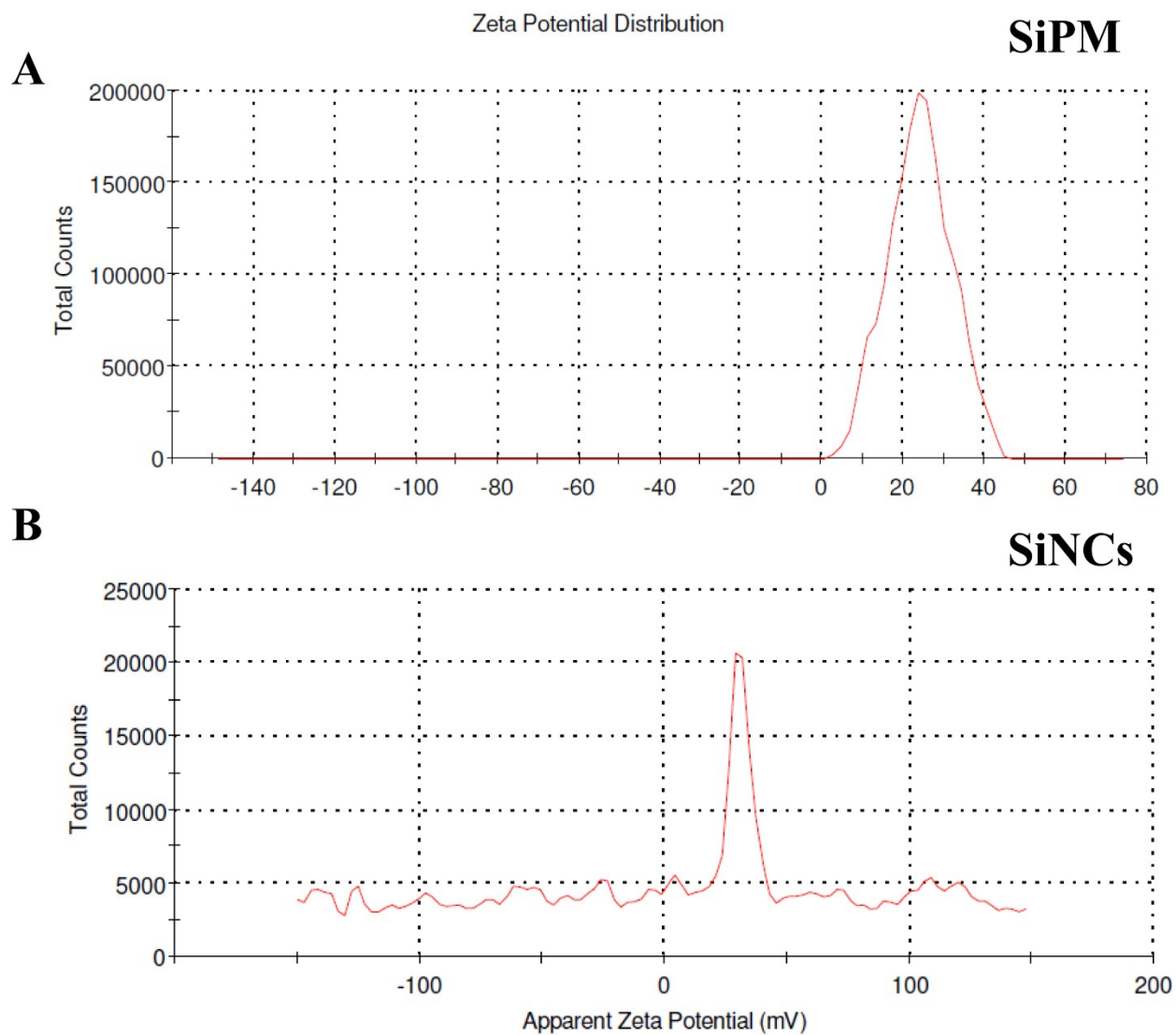
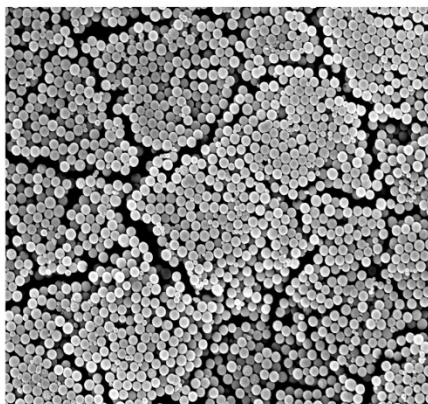
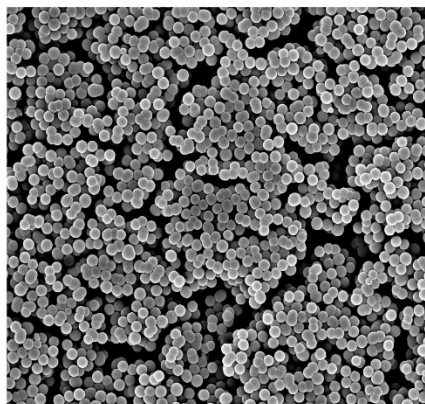


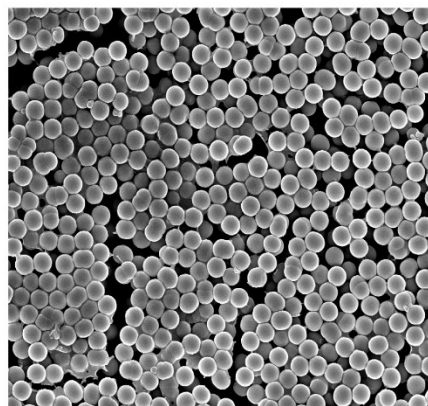
Fig. S4. Zeta potential measurement of (A)SiPM (~23mV) , and (B) hydrolytic silicon nanocrystals (SiNCs, ~29mV).

**A**

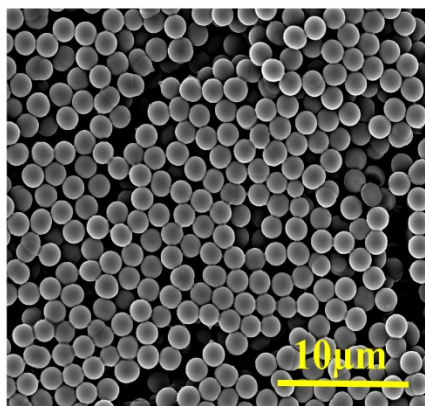
[APTES]=0.005  
[APTES]:[AA]≈3:1

**B**

[APTES]=0.011  
[APTES]:[AA]≈3:1

**C**

[APTES]=0.033  
[APTES]:[AA]≈3:1

**D**

[APTES]=0.055  
[APTES]:[AA]≈3:1

Fig. S5. SEM images of SiPM prepared at different APTES concentrations (M) in system. Scale bar is 10  $\mu\text{m}$  for all images.

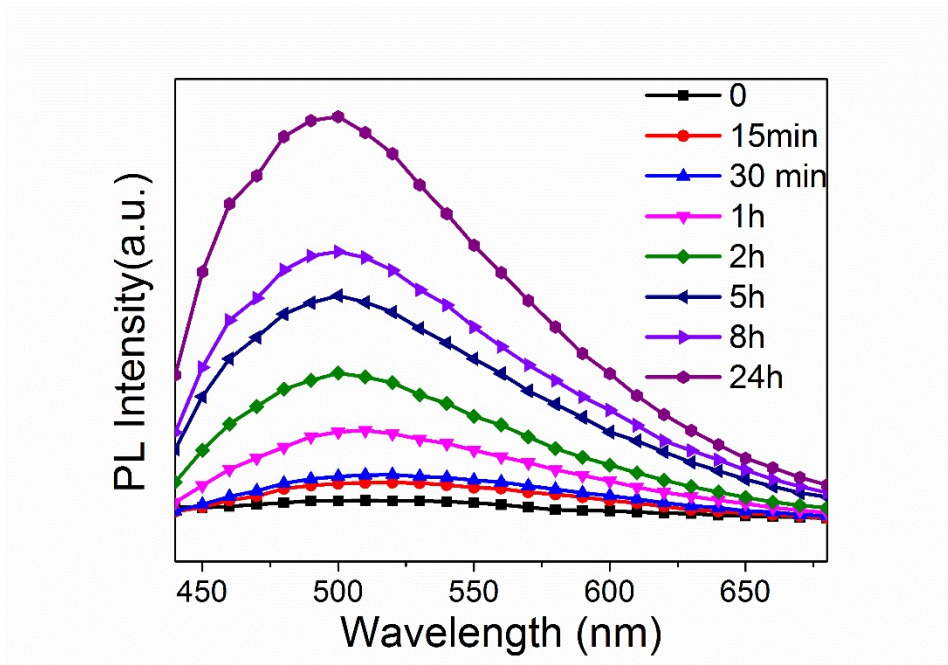


Fig. S6. The fluorescence spectra (excitation wavelength: 420nm) of SiPM with different reaction time.



Fig. S7. Digital pictures of SiPM with different reaction times.

**Table S1. Elemental composition of SiPM with different reaction time**

	C1s (%)	N1s (%)	O1s (%)	Si2p (%)
SiPM (30min)	48.57	10.47	29.70	11.26
SiPM (16h)	42.85	7.57	33.40	16.19

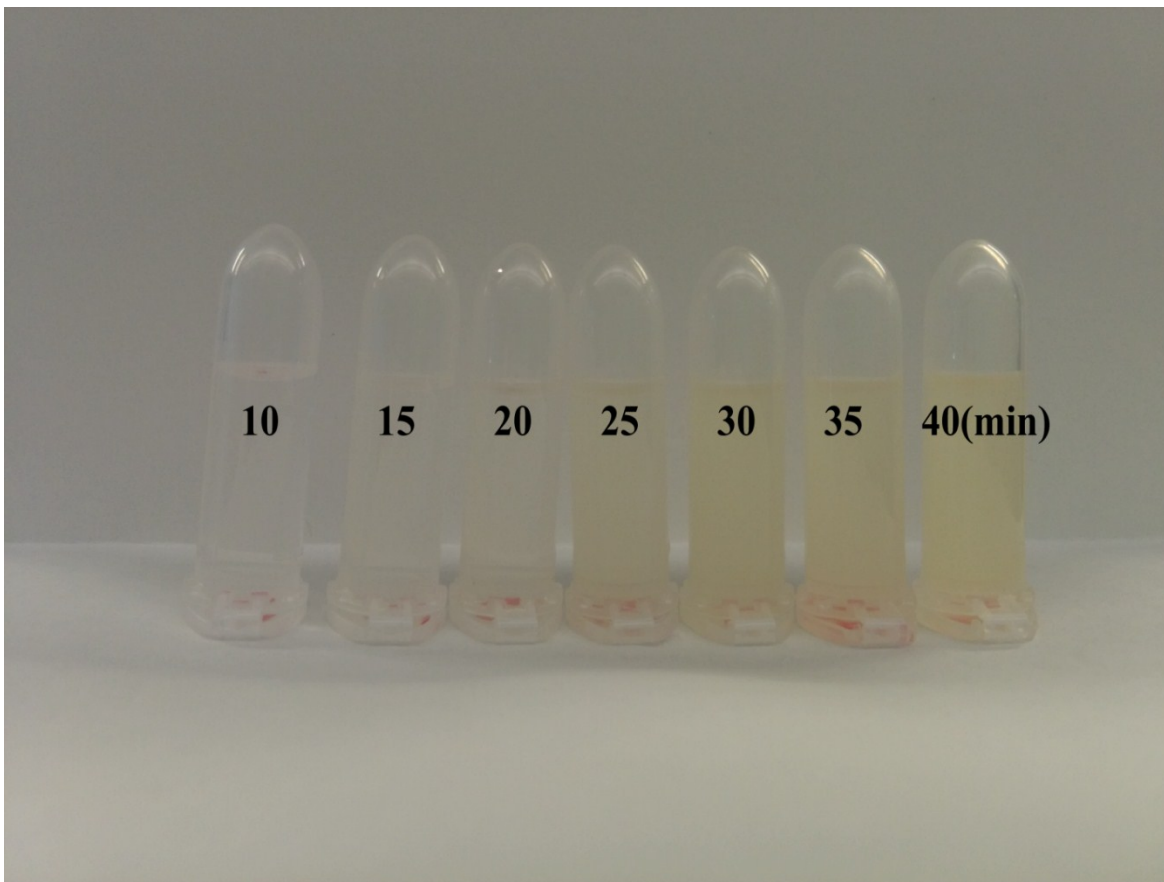


Fig. S8. Pictures of SiPM in tubes with increasing reaction time.

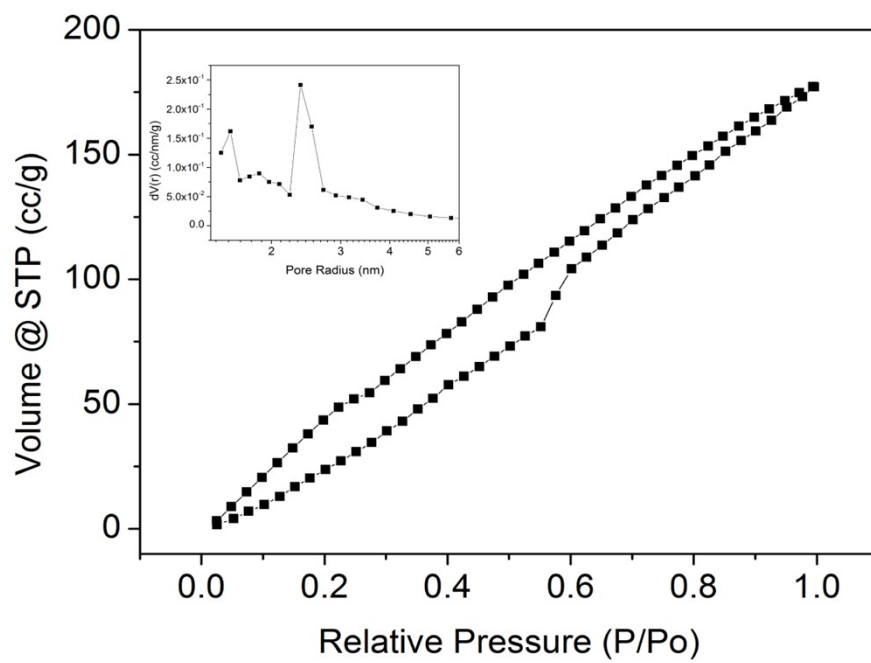


Fig. S9. N<sub>2</sub> adsorption/desorption isotherms of LD-SiPM (30min reaction time), inset displays Barrett-Joyner-Halenda (BJH) pore-size distribution curve obtained from the adsorption branch.

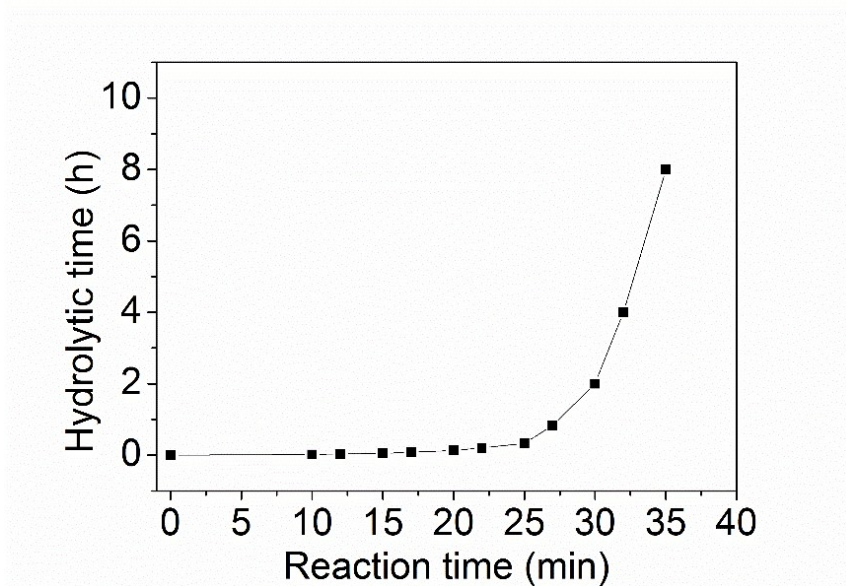


Fig. S10. Correlation of hydrolytic time of SiPM dispensed solutions (in PBS 7.4) with reaction time

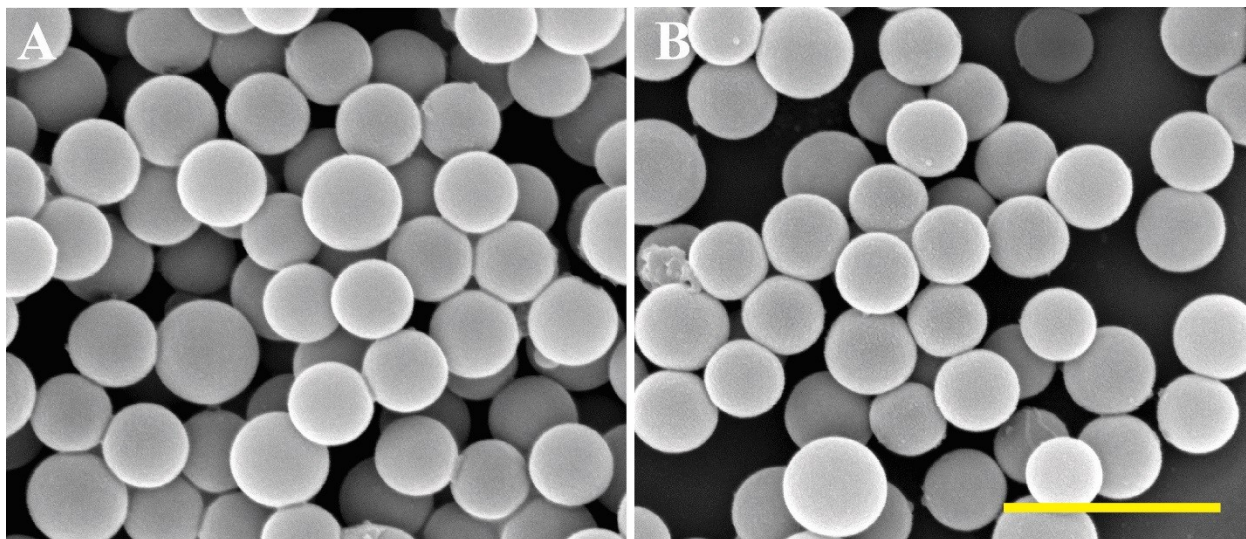


Fig. S11. SEM images of HD-SiPM after immersing in: (A) PBS (pH=7.4), and (B) water for three months.

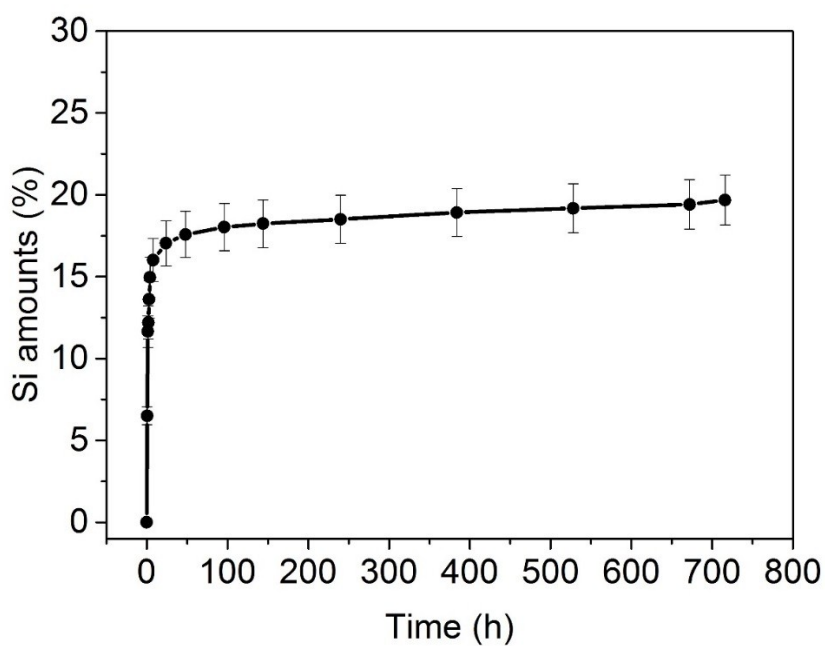


Fig. S12. Releasing curve of silicon elements (measured by ICP/OES) from SiPM (reaction time 1h) versus time in PBS (pH=7.4) at 37 °C.

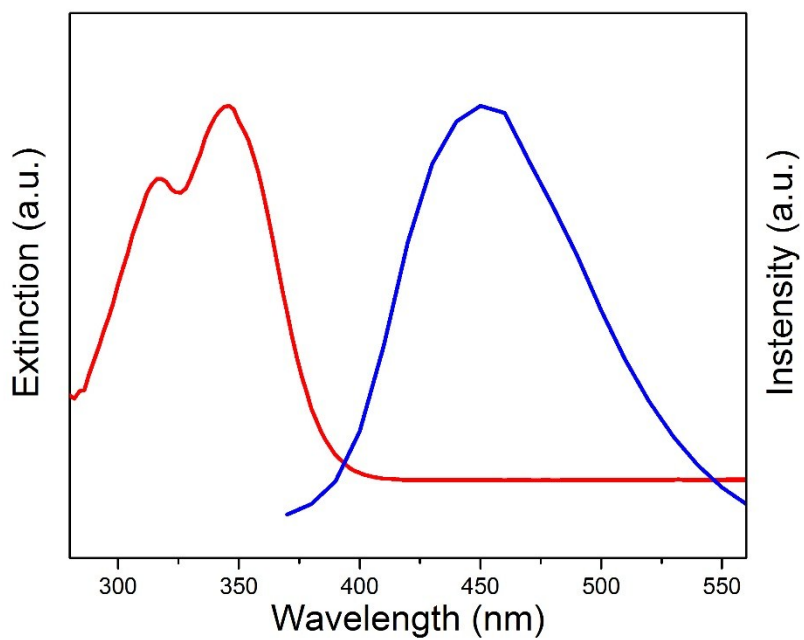


Fig. S13. UV-vis absorbance and photoluminescence curve of quinine sulfate.

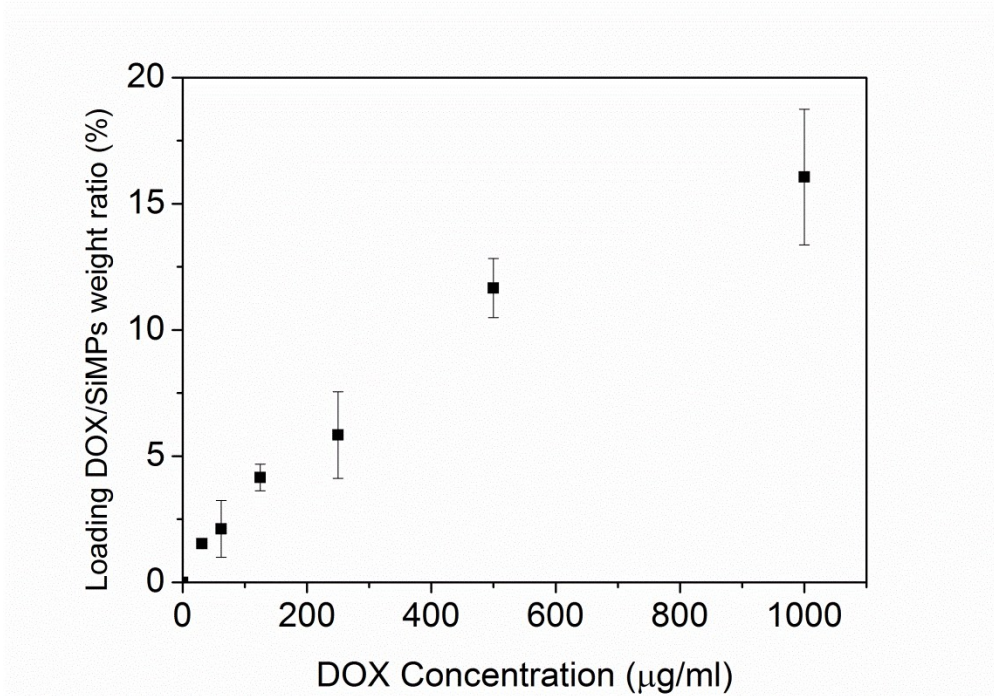
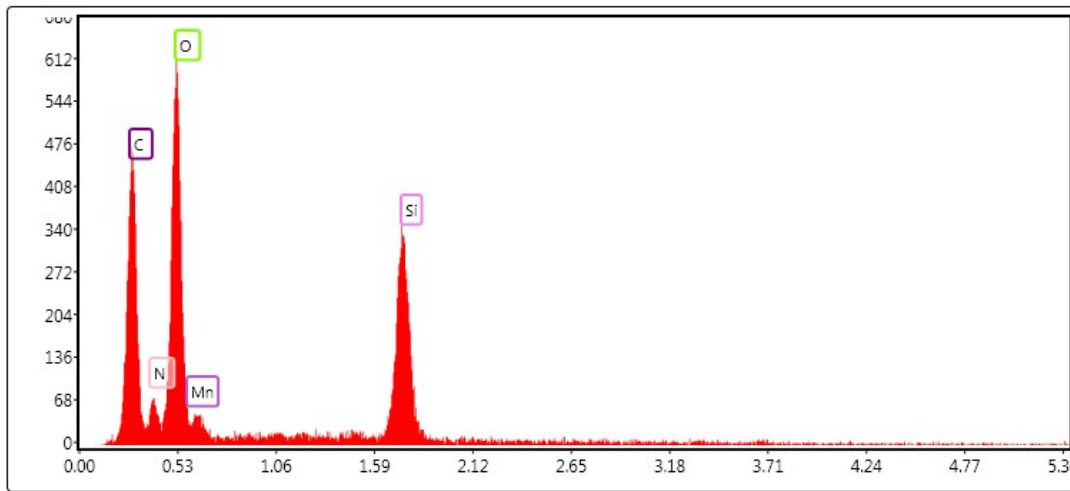


Fig. S14 Quantification of DOX loading in SiMP with various concentrations.



Status: Idle CPS: 0 DT: 0.0 Lsec: 30.0 19 Cnts 0.905 keV Det: Octane Super

Fig. S15. EDS spectrum of SiPM/MnO<sub>2</sub> composite

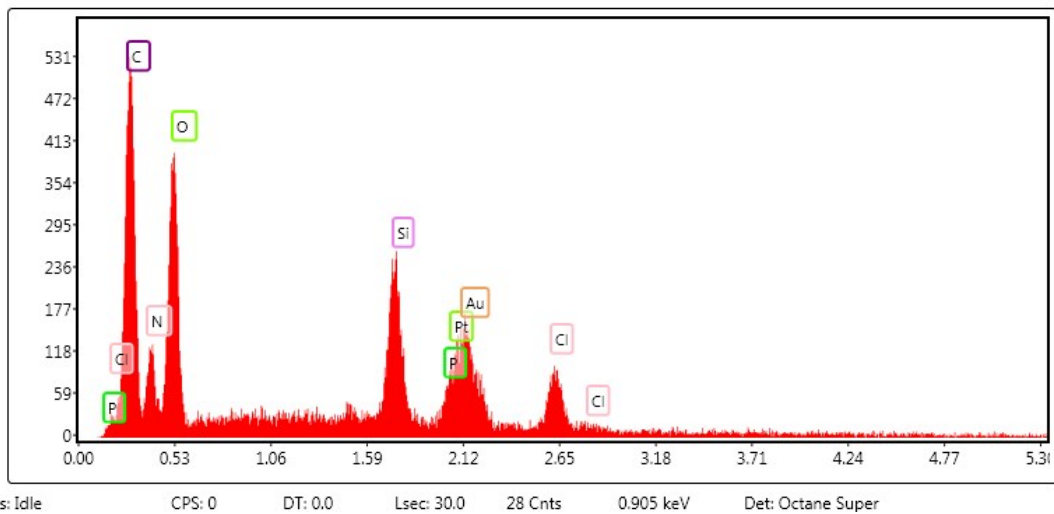


Fig. S16. EDS spectrum of SiPM/Au compisite

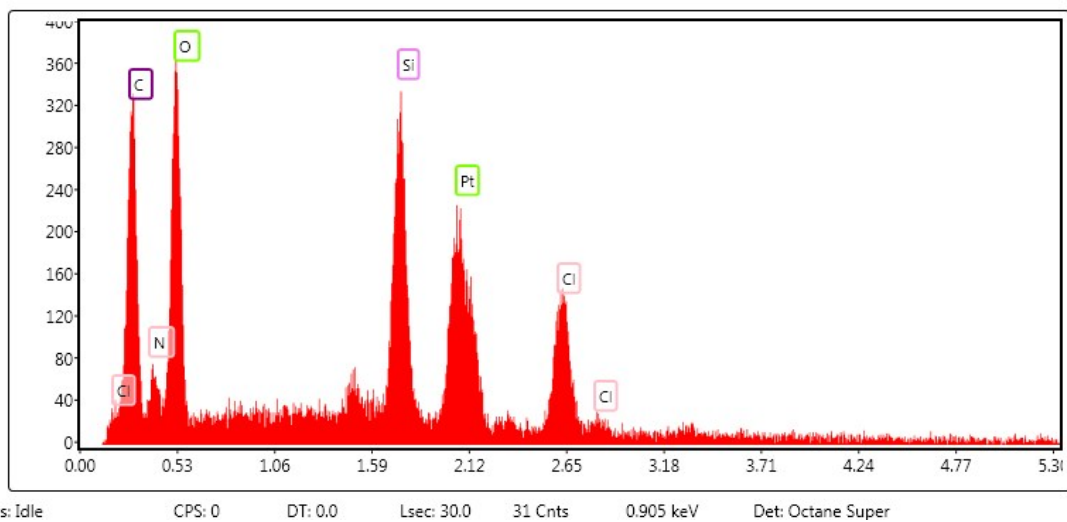


Fig. S17. EDS spectrum of SiPM/Pt compisite

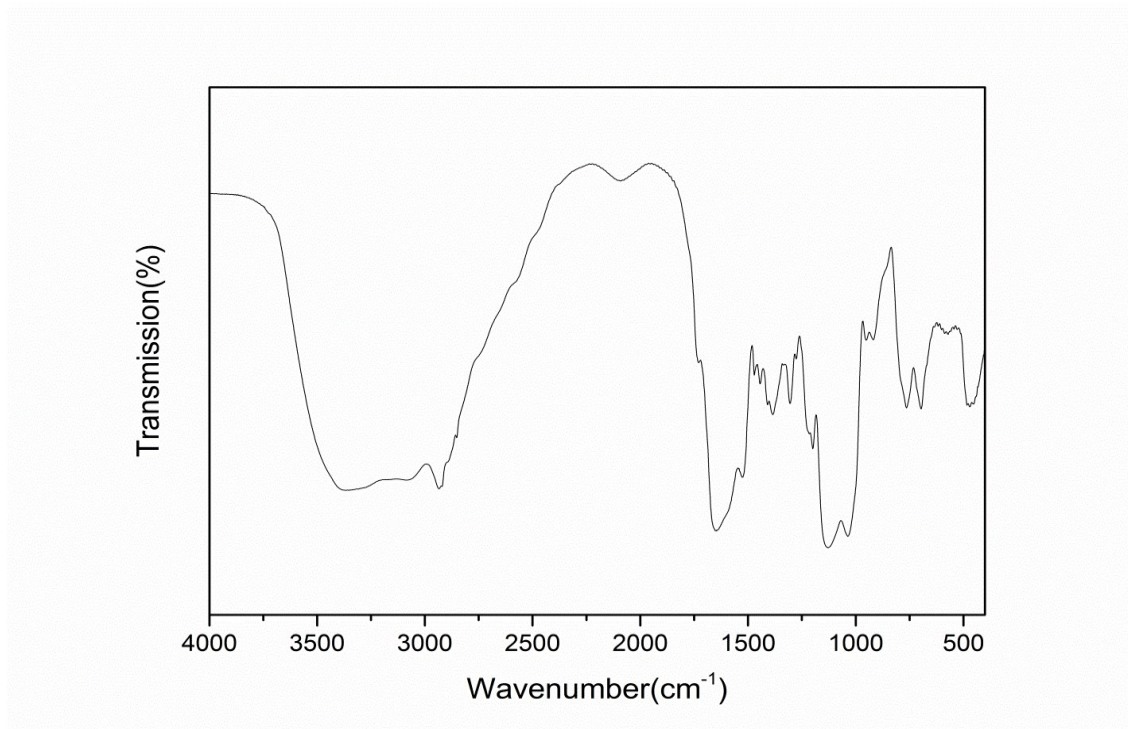


Fig. S18 FTIR spectrum of SiPM

The FTIR exhibits distinct peaks ranging from 1000 to 3500  $\text{cm}^{-1}$ . The peaks around 1000  $\text{cm}^{-1}$  and 1200  $\text{cm}^{-1}$  are characteristics of stretching vibrations of siloxane (Si-O-Si) groups. The absorbance peak at 2938  $\text{cm}^{-1}$  is due to C-H stretching. The broad peak between 3000  $\text{cm}^{-1}$  to 3600  $\text{cm}^{-1}$  stands for O-H stretching. The signals at 3400  $\text{cm}^{-1}$  and around 1637  $\text{cm}^{-1}$  are attributed to stretching and bending of N-H bond. Strong conjugates effects and hydrogen bonding could lower the frequency of C=O stretching vibration and enhance its absorbance. The sharp peak at 1637  $\text{cm}^{-1}$  would be the overlapping signals of N-H, C=C and C=O stretching vibrations.

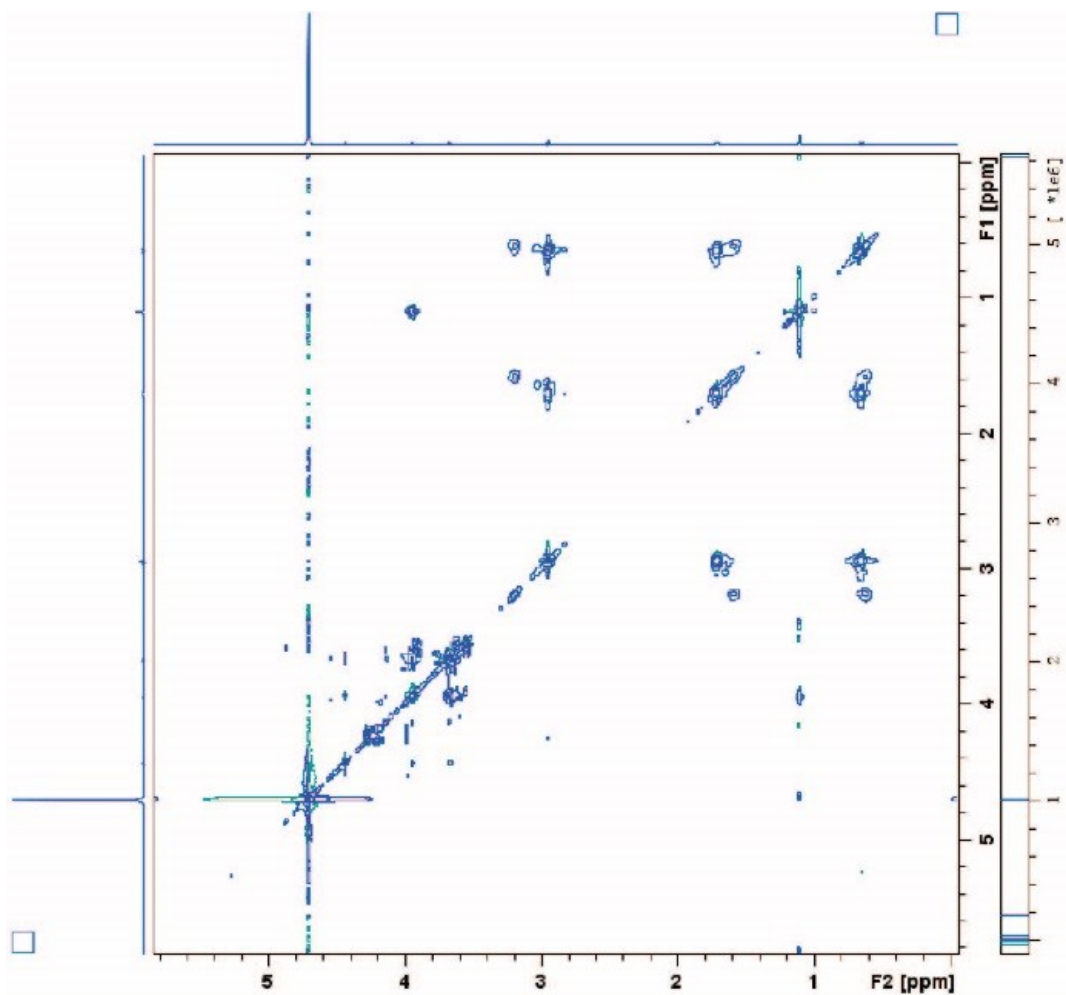


Fig. S19 2D TOCSY NMR spectrum of hydrolytic SiPM in D<sub>2</sub>O.

2D-TOCSY spectrum was measured in ordering to know the chemical structure of polymer matrices in SiPM. There is no obvious coupling between APTES and ascorbic acid. We supposed that the non-covalent bonding, electrostatic adherence or hydrogen bond might be the main bonding method in the polymer matrix in SiPM.

- (1) A. Shiohara, S. Hanada, S. Prabakar, K. Fujioka, T. H. Lim, K. Yamamoto, P. T. Northcote and R. D. Tilley, Chemical Reactions on Surface Molecules Attached to Silicon Quantum Dots. *J Am Chem Soc* **2010**, *132* (1), 248.
- (2) S. E. Lehman, Y. Tataurova, P. S. Mueller, S. V. S. Mariappan and S. C. Larsen, Ligand Characterization of Covalently Functionalized Mesoporous Silica Nanoparticles: An NMR Toolbox Approach. *J Phys Chem C* **2014**, *118* (51), 29943.
- (3) R. S. Reid, The Proton Nmr-Spectrum of Ascorbic-Acid - a Relevant Example of Deceptively Simple 2nd-Order Behavior. *J Chem Educ* **1989**, *66* (4), 344.